An Interplay Between Size and Electronic Effects in Determining the Homogeneity Range of the $A_9Zn_{4+x}Pn_9$ and $A_9Cd_{4+x}Pn_9$ Phases ($0 \le x \le 0.5$), A = Ca, Sr, Yb, Eu; Pn = Sb, Bi

Sheng-qing Xia and Svilen Bobev*

Department of Chemistry and Biochemistry, University of Delaware,

Newark, Delaware 19716

Content

6. Table S4. Atomic coordinates and isotropic displacement parameters (U_{eq}) for $A_9Cd_{4+x}Bi_9$ (A = Yb, Ca, Eu, Sr).

7. Table S5. Atomic coordinates and isotropic displacement parameters (U_{eq}) for $Yb_9Zn_{4.03(2)}Bi_9$ and $Ca_9Zn_{4.10(1)}Bi_9$.

8. Table S6. Atomic coordinates and isotropic displacement parameters (U_{eq}) $Sr_9Cd_{4.26(2)}Bi_9$, refined with allowing a small disorder around Bi2 (in order to account for the short Cd3–Bi2 distances – Table S7).

9. Table S7. Selected bond distances (Å) in $Sr_9Cd_{4.26(2)}Bi_9$, refined by two models: without and with allowing a small disorder around Bi2, respectively. See text for details

10. Figure S1. A view of the crystal structure of $Sr_9Cd_{4.49(1)}Sb_9$ projected approximately along the direction of the *c*-axis. Thermal ellipsoids are drawn at the 95% probability level. Color code: Sb – light blue full ellipsoids, Cd – purple crossed ellipsoids, Sr – red open ellipsoids.

11. Figure S2. Plots of the difference Fourier maps for $A_9Cd_{4+x}Bi_9$ (A = Yb, Ca, Eu, Sr). The height of the peak near Bi2 increases progressively as the occupancy of the interstitial cadmium site increases – the extra density can be modeled as statistically split Bi2A/Bi2B (see Table S7).

12. Figure S3. Temperature dependence of the resistivity of $Eu_9Cd_{4.21(1)}Bi_9$, measured by the four-probe method along the direction of the needle (*c*-axis). Data are normalized to the resistance value at room temperature. Four Platinum wires (0.002'') were attached to the samples using EPO-TEK H2O silver epoxy. A constant current of 1 mA was applied through the two outer leads and the voltages were measured across the inner two leads with the aid of a custom-built system. At each temperature, the voltage was measured twice (with reversed current directions) in order to subtract any thermoelectric voltages formed at the junctions of dissimilar materials. The room temperature resistivity is about 1.5 mΩ·cm.

Synthesis

$Sr_9Cd_{4.22(2)}Bi_9$

This compound was synthesized from an on-stoichiometry reaction in welded Nb tube. The best procedure is the following: Sr, Cd, and Bi were weighed out in a ratio of Sr : Cd : Bi = 9 : 4 : 9, loaded into Nb tube, which was subsequently arc-welded under argon. The reaction mixture was heated from room temperature to 1000°C at a rate of 200°/h, allowed to dwell at this temperature for 24 h, then subsequently cooled to 800°C at a rate of 3°/h. The 800°C temperature was kept for three days, after which the mixture was cooled to room temperature at a rate of 3°/h. Several other heat treatments were tried but despite all the efforts, the products of stoichiometric reactions always contained $Sr_{11}Bi_{10}$ as a secondary phase. Note that the same compound was made by the flux method (below); for the sake of easier comparison with the other bismuthides, the crystallographic data we refer to in the text are from the flux crystal grown .

$Yb_9Cd_{4.01(1)}Bi_9$, $Ca_9Cd_{4.06(1)}Bi_9$, $Sr_9Cd_{4.26(2)}Bi_9$

In these cases, the flux reactions proved more successful than the Nb tube reactions and provided an easier way to obtain these compounds in higher yields and at relatively lower temperatures. Using Cd as a self-flux was found to work the best in these systems. The typical procedures were as follows: the starting materials in a ratio of A : Cd : Pn = 9 : 40 : 9 (10-fold excess of Cd) were loaded in alumina crucibles, which were subsequently sealed in an evacuated fused silica jackets. The reaction mixtures were heated to 700°C at a rate of 200°/h, allowed to dwell at this temperature for 20 hours, and subsequently cooled slowly to 400°C at a rate of 3°/h. Then, the ampoule was taken out from furnace, inverted and placed into a centrifuge quickly to span for about 20-30 sec to

remove the excess of molten Cd. The typical products of such reactions were black and shiny needles of $A_9Cd_{4+x}Bi_9$ with very good diffraction quality. We note here that only the Sr-compound can be prepared with a reasonable success from "on-stoichiometry" reactions of the elements. All efforts to do so for the Yb and Cd analogs failed, the major products of such reactions were always $Yb_{11}Bi_{10}$ and $Ca_{11}Bi_{10}$.

$Eu_9Cd_{4.21(1)}Bi_9$.

For $Eu_9Cd_{4.21(1)}Bi_9$, the best synthetic procedure was a little different from above. The main product obtained using the nominal composition and the temperature profile for $Yb_9Cd_{4.01(1)}Bi_9$, $Ca_9Cd_{4.06(1)}Bi_9$, $Sr_9Cd_{4.26(2)}Bi_9$ was the new compound $Eu_{10}Cd_6Bi_{12}$ [*Chem. Asian J.* **2007**, *in print* - DOI : 10.1002/asia.200700016]. A second product of that reaction, albeit in small amounts, was the binary phase $EuCd_{11}$. Based on these observations, the reaction scheme was adjusted as follows: the starting materials were loaded in a ratio of Eu : Cd : Bi = 10 : 70 : 8 (*i.e.,* slightly richer in Eu and leaner in Bi in "more dilute" Cd solution) in an alumina crucible, which was subsequently sealed in an evacuated fused silica jacket. The reaction mixture was heated to 700°C at a rate of 200°C /h, allowed to dwell at this temperature for 20 hours, and subsequently cooled to 400°C at a rate of 3°C/h. After another dwelling step at this temperature for two days, the ampoule was then taken out from furnace, inverted and placed into a centrifuge quickly to span for about 20-30 sec to remove the excess of molten Cd. The main product of this reaction was $Eu_9Cd_{4.21(1)}Bi_9$ – nicely faceted and large needles. The new phase $Eu_{21}Cd_4Bi_{18}$ [$Sr_{21}Mn_4Sb_{18}$ structure type – unpublished work] was present as a secondary phase. The crystals from the latter were dark and irregularly shaped – the two phases were easy to separate under a microscope.

$Ca_9Zn_{4.10(1)}Bi_9$ and $Yb_9Zn_{4.03(2)}Bi_9$

The procedures for these Zn compounds are similar to those we employed for the Cd counterparts: the starting materials were loaded in a ratio of Ca (or Yb) : Zn : Bi = 9 : 40 : 9 in alumina crucibles, which were subsequently sealed in an evacuated fused silica jackets. The reaction mixture were heated from to 900°C (Zn has higher boiling point than Cd) at a rate of 300°C/h, allowed to dwell at this temperature for 20 hours, and subsequently cooled to 600°C at a rate of 5°C/h. Then, the ampoule was taken out from furnace, inverted and placed into a centrifuge quickly to span for about 20-30 sec to remove the excess of molten Zn. Lead flux was also successfully used for the synthesis of $Ca_9Zn_{4.10(1)}Bi_9$. The products from all flux reactions were black and shiny needles of the target compounds with good qualifications for single crystal diffraction. The details on growing related compounds in Zn flux can also be found in a previous article on $Ca_9Zn_{4+x}Sb_9$ and $Yb_9Zn_{4+x}Sb_9$.

Description of the positional disorder on the example of the structures of $A_9Cd_{4+x}Bi_9$

As mentioned already in the main text, the atomic distance between the interstitial site in $Sr_9Cd_{4.49(1)}Sb_9$, Cd3 and Sb2 is 2.593(3) Å, which is too short to be a "normal" Cd–Sb covalent bond. Such problems were also encountered in the previous report on the Zn counterparts ($Ca_9Zn_{4+x}Sb_9$ and $Yb_9Zn_{4+x}Sb_9$). Independent of the fact that Cd3 is far less than ¼ occupied, similarly short Zn–Bi and Cd–Bi contacts were found in all bismuth compounds too. We interpreted these abnormally short distances as an artifact of the low occupancy of the interstitial atom. After all, the majority (> 75%) of the pnicogen atoms are actually *not* bonded to the interstitial atom, Zn or Cd. In the minority case, when

there is an actual bond between these, a small "movement" of the immediate neighbors farther away from Cd3 (or Zn3) may allow for some extra room. To model this, a small positional disorder has to be taken into account and such assumption was proven reasonable and confirmed well by analyses of the Fourier maps calculated from low temperature single-crystal X-ray diffraction data for the series $Yb_9Cd_{4.01(1)}Bi_9$, $Ca_9Cd_{4.06(1)}Bi_9$, $Eu_9Cd_{4.21(1)}Bi_9$, and $Sr_9Cd_{4.26(2)}Bi_9$ (CSD numbers 417979, 417973, 417975, and 417976, respectively).

If we take the last member or this series as an example and calculate the distance between Cd3 and Bi2 in this compound, it is about 2.52(1) Å, apparently too short. The Fourier map (Figure S2) clearly shows that there is extra electron density near the Bi2 site in a direction exactly opposite the direction of the Cd3–Bi2 bond (Figure S2). To account for it, a small splitting of the Bi2 site can be introduced so that when Bi2 is at its "normal" position (87% of the time) Cd3 is missing. In the remaining 13% of the time, when Cd3 is there, Bi2 is pushed a bit away so that there is slightly more room for the interstitial atom. Relevant atomic coordinates, isotropic thermal parameters and distances refined using such a disorder model are given in Tables S6 and S7; a schematic presentation is given in the accompanying illustration. We also note that when the Cd3 (or Zn3) site has a lower occupancy, for example in the structures of $Yb_9Cd_{4.01(1)}Bi_9$, $Ca_9Cd_{4.06(1)}Bi_9$, $Yb_9Zn_{4.03(2)}Bi_9$ and even $Ca_9Zn_{4.10(1)}Bi_9$, such disorder becomes less prominent as there is virtually no electron density left near the Bi2 site (Figure S2).

Table S1. Selected crystallographic data and structure refinement parameters for $A_9Cd_{4+x}Bi_9$ (A = Yb, Ca, Eu, Sr).

Empirical formula	$Yb_9Cd_{4.01(1)}Bi_9$	$Ca_9Cd_{4.06(1)}Bi_9$	$Eu_9Cd_{4.21(1)}Bi_9$	$Sr_9Cd_{4.26(2)}Bi_9$[1]
Fw (g/mol)	3887.78	2697.88	3721.66	3143.73
Temperature (K)	120(2)			
Radiation	λ = 0.71073 Å, Mo Kα			
Crystal system	Orthorhombic			
Space group, Z	*Pbam* (No. 55), 2			
Unit cell dimensions (Å)	*a* = 22.426(3) *b* = 12.629(2) *c* = 4.7200(7)	*a* = 22.499(3) *b* = 12.708(2) *c* = 4.7229(7)	*a* = 23.162(2) *b* = 13.011(1) *c* = 4.8588(3)	*a* = 23.387(2) *b* = 13.191(1) *c* = 4.8916(4)
Volume (Å^3)	1336.8(3)	1350.4(3)	1464.3(2)	1509.1(2)
Density, ρ_{calc} (g/cm^3)	9.659	6.635	8.441	6.919
Absorption coeff. (mm^{-1})	93.183	63.219	75.752	70.886
Final R1 [I>2$\sigma_{(I)}$]	0.0367	0.0279	0.0266	0.0333
Final wR2 [I>2$\sigma_{(I)}$]	0.0731	0.0618	0.0552	0.0717
Largest peak/hole (e·Å^{-3})	2.972 / -3.332	3.417 / -2.255	3.485 / -3.433	3.689 / -2.630

[1] Data were also collected for a crystal of $Sr_9Cd_{4+x}Bi_9$ obtained from an "on-stoichiometry" reaction. The refined structure and unit cell constants (cell volume 1509.1(5) Å^3, refined formula $Sr_9Cd_{4.22(2)}Bi_9$, R1 = 0.0409 / wR2 = 0.0818) are in excellent agreement with the data from the flux-synthesized crystal. Unit cell constants in both cases deviate significantly from the previously reported ones (*a* = 23.47(2); *b* = 13.27(1); *c* = 4.89(1) Å – see Brechtel, E.; Cordier, G.; Schäfer, H. *Z. Naturforsch.* **1981**, *36B*, 1099-1104) suggesting either an abnormal and very anisotropic contraction of the cell parameters with the temperature or more likely, erroneous unit cell determination in the earlier report.

Table S2. Selected crystallographic data and structure refinement parameters for $Sr_9Cd_{4.49(1)}Sb_9$ synthesized by the flux method (lead flux).

Empirical formula	$Sr_9Cd_{4.49(1)}Sb_9$
Formula weight (g/mol)	2389.57
Temperature (K)	120(2)
Radiation	λ = 0.71073 Å, Mo Kα
Crystal system	Orthorhombic
Space group, Z	*Pbam* (No. 55), 2
Unit cell dimensions (Å)	*a* = 23.187(3) *b* = 13.064(3) *c* = 4.794(1)
Volume (Å^3)	1452(1)
Density, ρ_{calc} (g/cm^3)	5.464
Absorption coeff. (mm^{-1})	27.770
Final R1 [I>2$\sigma_{(I)}$] [a]	0.0307
Final wR2 [I>2$\sigma_{(I)}$] [a]	0.0633
Largest peak/hole (e·Å^{-3})	2.054 / -2.068

[a] $R_1 = \sum||F_o| - |F_c||/\sum|F_o|$; $wR_2 = [\sum[w(F_o^2 - F_c^2)^2]/\sum[w(F_o^2)^2]]^{1/2}$, where $w = 1/[\sigma^2F_o^2 + (0.015\cdot P)^2 + 16.49\cdot P]$, $P = (F_o^2 + 2F_c^2)/3$.

Table S3. Selected crystallographic data and structure refinement parameters for $Yb_9Zn_{4.03(2)}Bi_9$ and $Ca_9Zn_{4.10(1)}Bi_9$.

Empirical formula	$Yb_9Zn_{4.03(2)}Bi_9$	$Ca_9Zn_{4.10(1)}Bi_9$ [2]
Formula weight (g/mol)	3701.29	2508.90
Temperature (K)	120(2)	
Radiation	λ = 0.71073 Å, Mo Kα	
Crystal system	Orthorhombic	
Space group, Z	*Pbam* (No. 55), 2	
Unit cell dimensions (Å)	a = 21.997(3) b = 12.5243(14) c = 4.6283(5)	a = 22.0688(16) b = 12.5898(6) c = 4.6336(4)
Volume (Å^3)	1275.1(2)	1287.4(2)
Density, ρ_{calc} (g/cm^3)	9.640	6.472
Absorption coeff. (mm^{-1})	98.139	66.766
Final R1 [I>2$\sigma_{(I)}$]	0.0362	0.0174
Final wR2 [I>2$\sigma_{(I)}$]	0.0813	0.0394
Largest peak/hole (e·Å^{-3})	4.54 / -2.82	2.03 / -1.05

[2] Data were also collected for two more crystals of $Ca_9Zn_{4+x}Bi_9$ obtained from different reaction batches. The refinements in both cases are in excellent agreement with the data from the Zn flux-synthesized crystal (reported above). The nit cell constants at the same temperature (120 K) are as follows:

(1) Pb-flux grown crystal: cell volume 1287(1) Å^3;
a = 22.063(3), b = 12.593(2), c = 4.6327(7) Å, refined formula $Ca_9Zn_{4.09(2)}Bi_9$

(2) Zn-flux grown crystal: cell volume 1288(1) Å^3;
a = 22.071(4), b = 12.594(2), c = 4.6330(7) Å, refined formula $Ca_9Zn_{4.10(2)}Bi_9$

Table S4. Atomic coordinates and isotropic displacement parameters (U_{eq}) for $A_9Cd_{4+x}Bi_9$ (A = Yb, Ca, Eu, Sr).

Atoms	Wyckoff Site	*x*	*y*	*z*	U_{eq} (Å^2)	Occ.
$Yb_9Cd_{4.01(1)}Bi_9$ (CSD 417979)						
Bi1	2*d*	0	0.5	0.5	0.0083(3)	1
Bi2	4*g*	0.48864(4)	0.31850(7)	0	0.0098(2)	1
Bi3	4*g*	0.31373(4)	0.12062(7)	0	0.0097(2)	1
Bi4	4*h*	0.35584(4)	0.45594(7)	0.5	0.0087(2)	1
Bi5	4*h*	0.17236(4)	0.31756(7)	0.5	0.0089(2)	1
Yb1	2*b*	0	0	0.5	0.0099(3)	1
Yb2	4*g*	0.13609(5)	0.13339(8)	0	0.0096(2)	1
Yb3	4*g*	0.08921(5)	0.43320(8)	0	0.0098(2)	1
Yb4	4*g*	0.26644(5)	0.37558(8)	0	0.0108(2)	1
Yb5	4*h*	0.40003(5)	0.20836(8)	0.5	0.0107(2)	1
Cd1	4*h*	0.04753(8)	0.2677(1)	0.5	0.0107(4)	1
Cd2	4*h*	0.24109(8)	0.1129(2)	0.5	0.0116(4)	1
Cd3	4*g*	0.397(17)	0.37(3)	0	0.005	0.006(6)
$Ca_9Cd_{4.06(1)}Bi_9$ (CSD 417973)						
Bi1	2*d*	0	0.5	0.5	0.0127(2)	1
Bi2	4*g*	0.48911(2)	0.31794(4)	0	0.0146(2)	1
Bi3	4*g*	0.31354(2)	0.12143(4)	0	0.0144(1)	1
Bi4	4*h*	0.35570(2)	0.45627(4)	0.5	0.0129(1)	1
Bi5	4*h*	0.17200(2)	0.31673(4)	0.5	0.0130(1)	1
Ca1	2*b*	0	0	0.5	0.0149(8)	1
Ca2	4*g*	0.1358(1)	0.1333(2)	0	0.0156(6)	1
Ca3	4*g*	0.0896(1)	0.4358(2)	0	0.0158(6)	1
Ca4	4*g*	0.2663(1)	0.3758(2)	0	0.0181(6)	1
Ca5	4*h*	0.3994(1)	0.2094(2)	0.5	0.0172(6)	1
Cd1	4*h*	0.04708(5)	0.26983(8)	0.5	0.0149(2)	1

Cd2	4*h*	0.24084(5)	0.11313(8)	0.5	0.0167(2)	1
Cd3	4*g*	0.387(2)	0.354(3)	0	0.015(12)	0.029(5)
$Eu_9Cd_{4.21(1)}Bi_9$ (CSD 417975)						
Bi1	2*d*	0	0.5	0.5	0.0119(2)	1
Bi2	4*g*	0.49138(3)	0.31342(4)	0	0.0166(2)	1
Bi3	4*g*	0.30935(2)	0.12146(4)	0	0.0152(1)	1
Bi4	4*h*	0.35345(2)	0.45754(4)	0.5	0.0122(1)	1
Bi5	4*h*	0.16904(2)	0.31410(4)	0.5	0.0118(1)	1
Eu1	2*b*	0	0	0.5	0.0133(2)	1
Eu2	4*g*	0.13660(3)	0.13435(6)	0	0.0138(2)	1
Eu3	4*g*	0.08918(3)	0.43557(6)	0	0.0130(2)	1
Eu4	4*g*	0.26303(3)	0.37621(6)	0	0.0164(2)	1
Eu5	4*h*	0.39830(3)	0.20837(6)	0.5	0.0168(2)	1
Cd1	4*h*	0.04607(4)	0.27074(8)	0.5	0.0143(2)	1
Cd2	4*h*	0.24058(5)	0.11622(8)	0.5	0.0153(2)	1
Cd3	4*g*	0.3878(4)	0.3644(8)	0	0.015(3)	0.105(5)
$Sr_9Cd_{4.26(2)}Bi_9$ (CSD 417976)						
Bi1	2*d*	0	0.5	0.5	0.0138(3)	1
Bi2	4*g*	0.49213(4)	0.31146(7)	0	0.0181(2)	1
Bi3	4*g*	0.30792(4)	0.12141(7)	0	0.0174(2)	1
Bi4	4*h*	0.35314(4)	0.45764(6)	0.5	0.0139(2)	1
Bi5	4*h*	0.16802(4)	0.31172(6)	0.5	0.0136(2)	1
Sr1	2*b*	0	0	0.5	0.0154(6)	1
Sr2	4*g*	0.13608(9)	0.1336(2)	0	0.0150(4)	1
Sr3	4*g*	0.08945(9)	0.4375(2)	0	0.0151(4)	1
Sr4	4*g*	0.2626(1)	0.37554(2)	0	0.0196(5)	1
Sr5	4*h*	0.39749(9)	0.2094(2)	0.5	0.0202(5)	1
Cd1	4*h*	0.04547(7)	0.2732(1)	0.5	0.0169(4)	1
Cd2	4*h*	0.24000(7)	0.1155(1)	0.5	0.0174(4)	1
Cd3	4*g*	0.3895(5)	0.369(1)	0	0.022(4)	0.13(1)

Table S5. Atomic coordinates and isotropic displacement parameters (U_{eq}) for $Yb_9Zn_{4.03(2)}Bi_9$ and $Ca_9Zn_{4.10(1)}Bi_9$.

Atoms	Wyckoff Site	*x*	*y*	*z*	U_{eq} (Å^2)	Occ.
$Yb_9Zn_{4.03(2)}Bi_9$ (CSD 417977)						
Bi1	2*d*	0	0.5	0.5	0.0138(2)	1
Bi2	4*g*	0.49253(3)	0.31021(5)	0	0.0143(1)	1
Bi3	4*g*	0.30736(3)	0.11457(5)	0	0.0143(1)	1
Bi4	4*h*	0.35455(3)	0.45400(5)	0.5	0.0138(1)	1
Bi5	4*h*	0.17040(3)	0.30875(5)	0.5	0.0137(1)	1
Yb1	2*b*	0	0	0.5	0.0140(2)	1
Yb2	4*g*	0.13809(3)	0.13115(5)	0	0.0143(1)	1
Yb3	4*g*	0.08921(3)	0.42817(6)	0	0.0144(1)	1
Yb4	4*g*	0.26506(3)	0.37277(5)	0	0.0146(1)	1
Yb5	4*h*	0.39918(3)	0.20471(5)	0.5	0.0146(1)	1
Zn1	4*h*	0.04749(10)	0.27061(16)	0.5	0.0155(4)	1
Zn2	4*h*	0.23844(10)	0.11035(16)	0.5	0.0151(4)	1
Zn3	4*g*	0.377(9)	0.376(1)	0	0.010	0.014(8)
$Ca_9Zn_{4.10(1)}Bi_9$ (CSD 417978)						
Bi1	2*d*	0	0.5	0.5	0.0129(2)	1
Bi2	4*g*	0.49282(3)	0.30943(4)	0	0.0139(2)	1
Bi3	4*g*	0.30693(3)	0.11601(4)	0	0.0139(2)	1
Bi4	4*h*	0.35430(3)	0.45447(4)	0.5	0.0129(1)	1
Bi5	4*h*	0.16963(3)	0.30805(4)	0.5	0.0126(1)	1
Sr1	2*b*	0	0	0.5	0.0145(8)	1
Sr2	4*g*	0.13747(15)	0.1310(2)	0	0.0147(5)	1
Sr3	4*g*	0.08974(15)	0.4307(2)	0	0.0161(6)	1
Sr4	4*g*	0.26471(15)	0.3733(2)	0	0.0166(6)	1
Sr5	4*h*	0.39858(15)	0.2058(2)	0.5	0.0162(6)	1
Zn1	4*h*	0.04686(9)	0.27267(14)	0.5	0.0150(3)	1
Zn2	4*h*	0.23809(9)	0.11111(14)	0.5	0.0151(3)	1
Zn3	4*g*	0.3888(8)	0.3675(15)	0	0.015(7)	0.051(5)

Table S6. Atomic coordinates and isotropic displacement parameters (U_{eq}) $Sr_9Cd_{4.26(2)}Bi_9$, refined with allowing a small disorder around Bi2 (in order to account for the short Cd3–Bi2 distances – Table S7).

Atoms	Wyckoff Site	*x*	*y*	*z*	U_{eq} (Å^2)	Occ.
Bi1	2*d*	0	0.5	0.5	0.0139(3)	1
Bi2A	4*g*	0.4907(1)	0.3122(2)	0	0.0145(4)	0.87
Bi2B	4*g*	0.5038(7)	0.3056(10)	0	0.0145(4)	0.13
Bi3	4*g*	0.3079(1)	0.1214(1)	0	0.0174(2)	1
Bi4	4*h*	0.3531(1)	0.4576(1)	0.5	0.0140(2)	1
Bi5	4*h*	0.1680(1)	0.3117(1)	0.5	0.0137(1)	1
Sr1	2*b*	0	0	0.5	0.0155(6)	1
Sr2	4*g*	0.1381(1)	0.1336(2)	0	0.0152(4)	1
Sr3	4*g*	0.0895(1)	0.4375(2)	0	0.0152(1)	1
Sr4	4*g*	0.2626(1)	0.3755(2)	0	0.0197(5)	1
Sr5	4*h*	0.3975(1)	0.2094(1)	0.5	0.0202(5)	1
Cd1	4*h*	0.0455(1)	0.2732(1)	0.5	0.0169(3)	1
Cd2	4*h*	0.2400(1)	0.1155(1)	0.5	0.0175(4)	1
Cd3	4*g*	0.3895(5)	0.3688(11)	0	0.022(4)	0.13(1)

Table S7. Selected bond distances (Å) in $Sr_9Cd_{4.26(2)}Bi_9$, refined by two models: without and with allowing a small disorder around Bi2, respectively. See text for details.

Model without Bi2 disorder		**Model with Bi2 disorder**	
Bonds	**Distances (Å)**	**Bonds**	**Distances (Å)**
Cd1–Bi1	3.174(2)	Cd1–Bi1	3.174(2)
Cd1–Bi2 × 2	2.964(1)	Cd1–Bi2A × 2	2.981(2)
		Cd1–Bi2B × 2	2.830(8)
Cd1–Bi5	2.913(2)	Cd1–Bi5	2.912(2)
Cd2–Bi3 × 2	2.918(1)	Cd2–Bi3 × 2	2.918(1)
Cd2–Bi4	3.014(2)	Cd2–Bi4	3.014(2)
Cd2–Bi5	3.087(2)	Cd2–Bi5	3.087(2)
Cd3–Bi2	2.52(1)	Cd3B–Bi2B	2.80(2)
Cd3–Bi4 × 2	2.841(7)	Cd3B–Bi4 × 2	2.842(7)

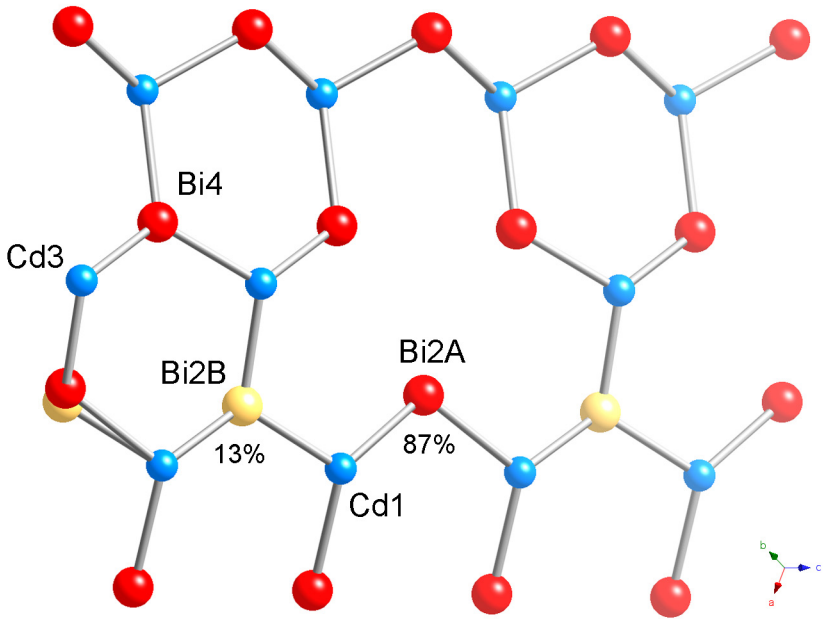

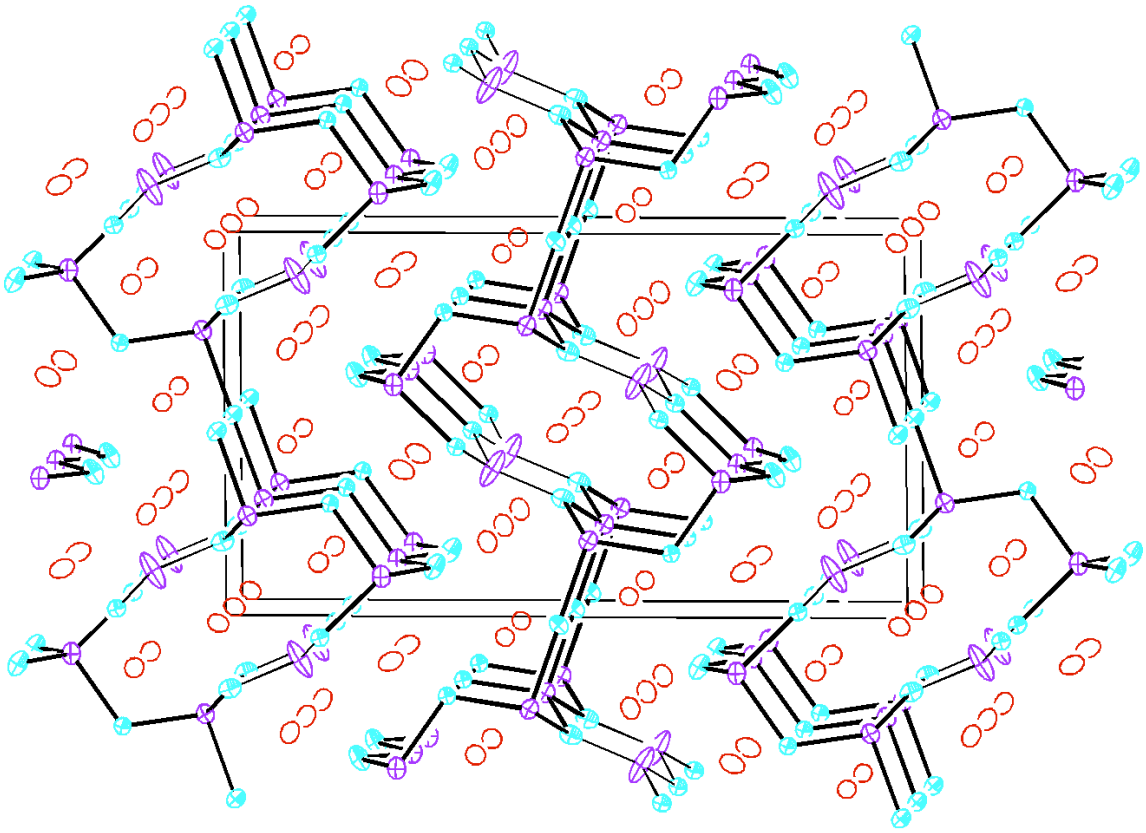

Figure S1. A view of the crystal structure of $Sr_9Cd_{4.49(1)}Sb_9$ projected approximately along the direction of the *c*-axis. Thermal ellipsoids are drawn at the 95% probability level. Color code: Sb – light blue full ellipsoids, Cd – purple crossed ellipsoids, Sr – red open ellipsoids.

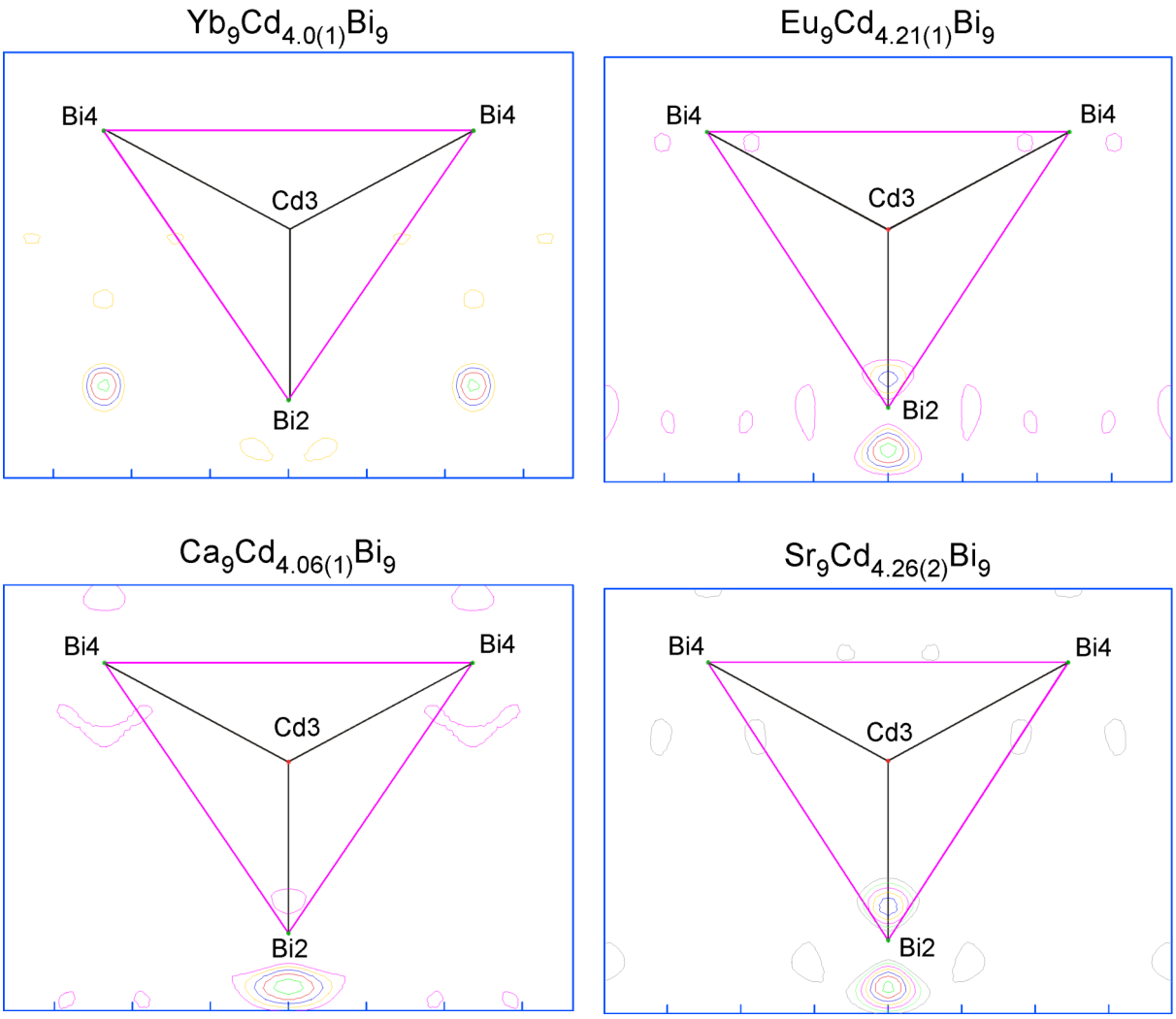

Figure S2. Plots of the difference Fourier maps for $A_9Cd_{4+x}Bi_9$ (A = Yb, Ca, Eu, Sr). The height of the peak near Bi2 increases progressively as the occupancy of the interstitial cadmium site increases – the extra density can be modeled as statistically split Bi2A/Bi2B (see Table S7).

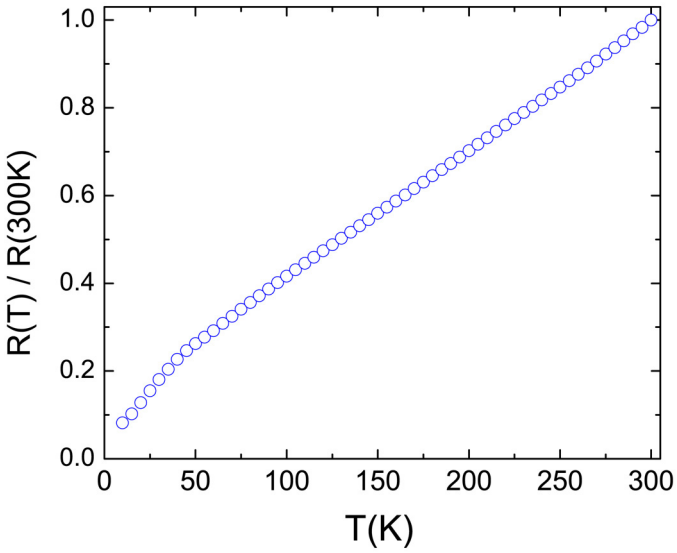

Figure S3. Temperature dependence of the resistivity of $Eu_9Cd_{4.21(1)}Bi_9$, measured by the four-probe method along the direction of the needle (*c*-axis). Data are normalized to the resistance value at room temperature. Four Platinum wires (0.002'') were attached to the samples using EPO-TEK H2O silver epoxy. A constant current of 1 mA was applied through the two outer leads and the voltages were measured across the inner two leads with the aid of a custom-built system. At each temperature, the voltage was measured twice (with reversed current directions) in order to subtract any thermoelectric voltages formed at the junctions of dissimilar materials. The room temperature resistivity is about 1.5 mΩ·cm.